FIBRE DISTRIBUTION INSIDE YARNS OF TEXTILE COMPOSITE: GEOMETRICAL AND FE MODELLING

V. Koissin[*]*, D.S. Ivanov, S.V. Lomov, I. Verpoest*
Dept. of Metallurgy and Materials Engineering, Katholieke Universiteit Leuven,
Kasteelpark Arenberg 44, B–3001 Leuven, Belgium
[*]*Vitaly.Koysin@mtm.kuleuven.be*

ABSTRACT

This article addresses the experimental investigation and modelling of the uneven fibre distribution inside yarns of a textile composite. The test data is given for the tri-axial carbon-fibre braid; a considerable irregularity is revealed for the fibre distribution along and across the yarns. The importance of this effect for the damage resistance is illustrated with a simple finite-element (FE) model. The geometrical modelling of the internal geometry is also discussed.

INTRODUCTION

Optimised design methods facilitate an extensive use of textile composites in load-bearing components for different applications. However, being a quite modern design concept, it is relatively unexplored and employed with caution. Due to a natural complex structure and manufacture methods, a textile composite contains resin-rich zones, uneven fibre content, etc. These features raise concerns about the damage resistance, which is closely connected with the reinforcement internal geometry and reveals features not observed in the classical laminates (1–4). Hence, whilst the design for the stiffness of a textile composite part can be based on validated calculation techniques, related to the meso-structure of textile reinforcements, the reliable strength design has to be based on empirical information (5) and should account for the micro-structure. This paper focuses on the uneven fibre distribution inside the textile yarns. The object to study is one of basic types of the textile reinforcement — multi-layer preform made of 2D braided carbon-fibre yarns. The braid is considered as a complex hierarchical structure. Its meso-level includes the variable fibre content along the yarn; this scale naturally corresponds to the unit cell size. The micro-level embraces the uneven fibre distribution over the yarn cross-section.

EXPERIMENTAL STUDY

Materials

Tri-axial (+45°, 0°, -45°) HTS 5631 Tenax carbon fibre braid was used as the composite reinforcement, Fig. 1(a). The fabric was composed of 2 braiding and 1 inlay yarns made of the same 12 K tows with the linear density of 1600 tex. The average yarn width was 4.2 or 3.7 mm, respectively. The braiding yarns were organised in so-called diamond pattern 1/1 with the braiding angle of $91.1 \pm 1.3°$. The length of the unit cell side was 14.4 mm (sides were parallel to the braiding yarns). The basic properties of the fibres are listed in Table 1. Four layers of the fabric were put in a pile with the equal layup direction, i.e. a transversely orthotropic $[+45,0,–45]_4$ construction was produced. The layers were shifted as shown in Figs. 1(b)–1(d).

The resin transfer moulding (RTM) equipment was employed for the impregnation. The preform was placed into a flat mold warmed up at 40°C. Shell epoxy resin 828 LV and hardener DX 6514 were used with the mix ratio of 100:17. The resin was injected into the vacuumized mould under the differential pressure of 2–3 bars. When a complete impregnation was observed through the transparent mould cover (after ≈25 min), the cure stage was processed for 1 hour with the temperature of 70°C. After demoulding, the composite plate was post-cured in an air

Table 1: Characteristics of the carbon fibres (6).

diameter, μm	density, kg/m^3	Young's modulus, GPa	shear modulus, GPa	Poisson's ratio	tensile strength, MPa
7	1760	238	24	0.23	4300

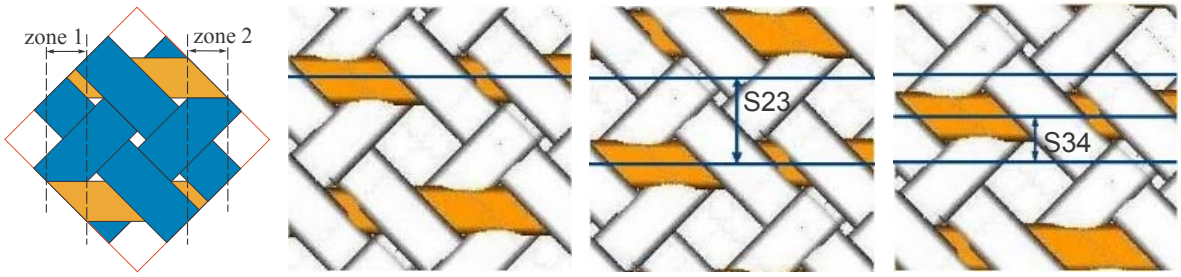

(a) unit cell (b) 1st and 2nd layers (c) 3rd layer (d) 4th layer

Figure 1: Unit cell (a) and shifts between layers (b–d): no shift for first two layers, S23=4.7 mm — between the 2nd and the 3rd layers, S34=4.7 mm — between the 3rd and the 4th layers.

oven at 160°C for another hour. The final thickness of the plate was 3.1 mm; the average fibre volume fraction was estimated to be about 43%. The areal weight of the plate was 600 g/m^2.

Meso-geometry of the preform

To investigate the preform's internal structure after the RTM, series of specimens were sectioned across the inlays and polished to allow for inspection with an optical or electron microscope. Typical through-the-thickness micrograph is shown in Fig. 2(left). A high deformation of the yarns is seen; this effect can be attributed to a severe compression during the RTM process.
In order to assess the fibre volume fraction in the inlay yarns, a number of the micrographs was investigated. First, the area of each inlay cross-section was calculated approximately. Then, knowing the number of filaments and their diameter, Table 1, the average fibre volume fraction was easily obtained for each position. The results are shown in Fig. 2(right), which illustrates the fibre volume fraction distribution along the inlay yarns. A prominent (about 10%) rise is seen nearby the area of nesting with the braiding yarns. The distribution is not symmetrized.

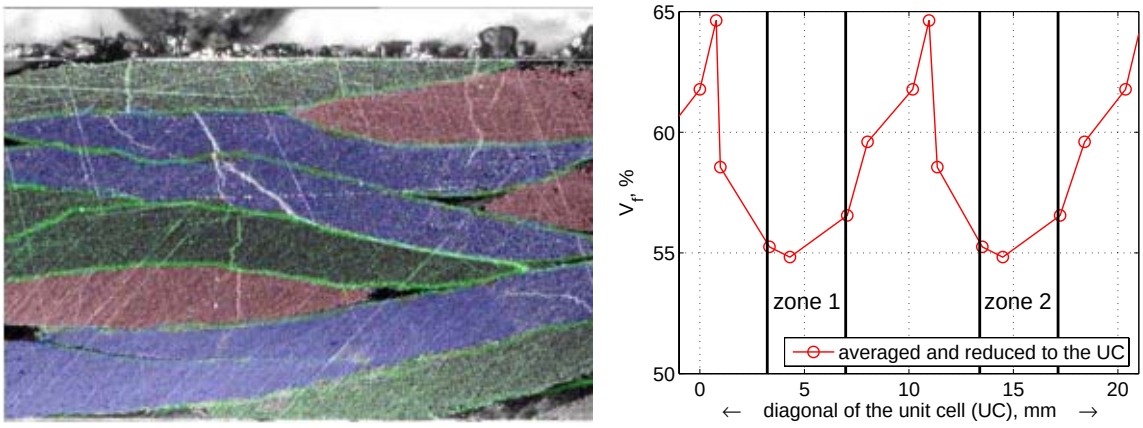

Figure 2: Micrograph of the cross-section cut across the inlay yarns (left, colors are implied manually) and measured distribution of the fibre volume fraction along the inlays (right, (7)).

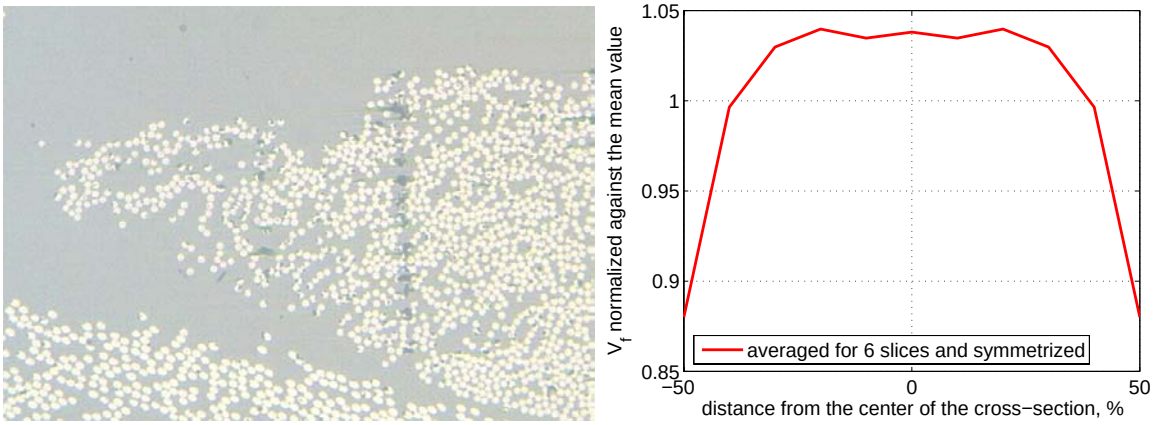

Figure 3: Typical micrograph of the cross-section cut across the inlay yarns (left, only the yarn edge is shown) and measured distribution of the fibre volume fraction across the inlays (right).

Micro-geometry of the preform

It is a well-known fact that the multifilament yarns have a non-uniform fibre distribution over the cross-section. The fibre content usually decreases towards the edge of a yarn; however, the maximum can be observed somewhere in between the centre and edge (8). In the preform, then, the braiding process, nesting in the mould, etc. changes the virgin distribution of the fibre volume fraction. Figure 3(left) shows a typical microscope image of the fibre placement at the yarn edge. It is clearly seen that the local fibre content is lower near the edge.

The statistical data is obtained taking micrographs with the SEM, stitching them automatically into one image, extracting small sub-images across the yarn, black & white thresholding, and calculating the fibre area in a Matlab applet. The results are shown in Fig. 3(right), which illustrates the fibre volume fraction distribution across the inlay yarns; the distribution is normalized against its average value (59%). A prominent (about 15%) decrease is seen nearby the edges; this observation is in agreement with the data reported by other authors (1, 2, 8) for fibrous bundles in woven fabrics. In Ref. (2), it is shown also that the fibre fraction may vary not only along the bundle cross-section but also across it (again, with lower fraction at the edge).

MODELLING

Geometrical modelling

The geometrical modelling is performed using the textile simulating software WiseTex. Figures 1(b)–1(d) show the results; comparison with the photos of the real fabric (6, 7) reveals that the model captures its important features. Unfortunately, although due to inherent properties of the geometrical approach, the simplifying assumption of idealized (elliptic in the present case) yarn cross-section is coded in the WiseTex. Therefore, the yarn nesting is modelled not perfectly, and some local intersections of the yarns can be observed as seen in Figs. 1(b)–1(d). Since distortion of the shape of the cross-section can not exactly be modelled without an FE analysis, a rotation of the yarns is introduced for a more realistic description. As a result, the intersection of the yarns decreases considerably. However, it is not eliminated completely; the remaining penetration represents an error of the current geometrical modelling (9).

In the braids with inlays, axial yarns are inlaid between the braided yarns in the machine direction. Study of the geometry of tri-axial braids (10) reveals almost no crimp for axial yarns (inlays). This is logical for balanced braids, as the one used in the present study. If a braid is

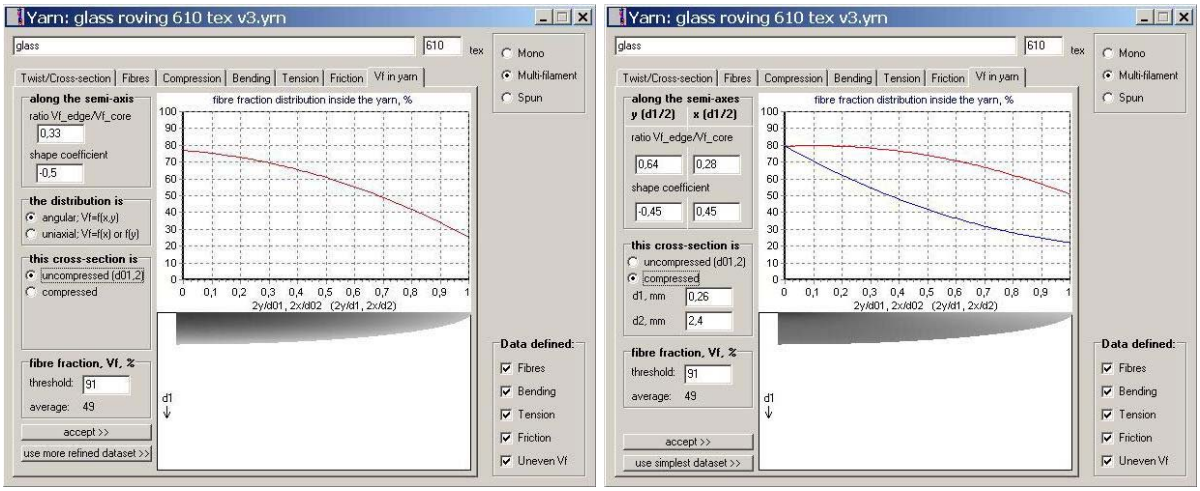

Figure 4: WiseTex dialogue window for the modelling of the local fibre distribution in a yarn. Left — uniaxial case, right — biaxial case of the distribution. For the better view, the yarn dimensions and the fibre distribution do not correspond to the braid configuration and internal structure discussed in the present study.

unbalanced (which is a rare case in practice), then the crimp of inlays, fixed between the two systems of braiding yarns and therefore prevented from a significant bending, must be quite low also. Reasoning from these considerations and the experimental evidence, it is usually assumed in the WiseTex algorithms that the inlays are perfectly straight. However, some crimp of the inlays can also be modelled, if necessary. In a simulated laminate (LamTex software), when several layers of the braid are nested together, the inlays are supposed to keep the crimp created by the WiseTex. In the real laminate, certain crimp is also observed for the inlays (7).

Once the geometrical model is built, the fibre distribution inside the yarns is modelled to produce a complete description of the unit cell fibrous structure. In the simplest case, such a model assumes the even fibre placement over the cross-sections, taking into account only the variability along the yarn due to its compression by the nesting forces. On the programme request, the local fibre volume fraction and the fibre orientation are generated for any point inside the unit cell. Particularly, the fibre content can be zero, if the point does not lie inside a yarn.

Alternatively, the refined model of the local fibre distribution can be employed. For the present case of the flattened yarn, the unidirectional fibre distribution is modelled, when the fibre content changes only at the long axis of the elliptic cross-section. The distribution is given with the 2nd-order polynomial using two parameters 1) ratio between the fibre content at the core (mechanical centre) and edge of the yarn and 2) shape coefficient. The function is normalized automatically with the weight factor, which implies that the average fibre volume fraction equals to the one obtained using the number of fibres, their diameter, and the total area of the yarn's cross-section. In a general case, if the fibre distribution is not unidirectional, the options of angular or "biaxial" distribution can be used in the WiseTex. The examples are shown in Fig. 4.

When calculating the compressed state of a yarn, in the case of need, the polynomial is changed automatically to fit the average fibre fraction in the compressed yarn. If possible, only the weight factor is changed in this case; otherwise, the function is flattened reducing the shape coefficient to zero and approaching the core-to-edge ratio to unity. In the limit case, the auto-correction of the fibre distribution leads to the uniform compaction, when the average fibre content reaches its threshold value. On default, the hexagonal grid packing of uncompressible equal cylindrical fibres is assumed that yields that the maximal fibre content can not exceed 91%.

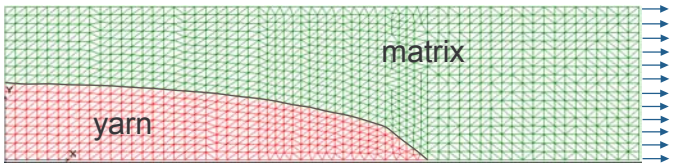

Figure 5: FE model.

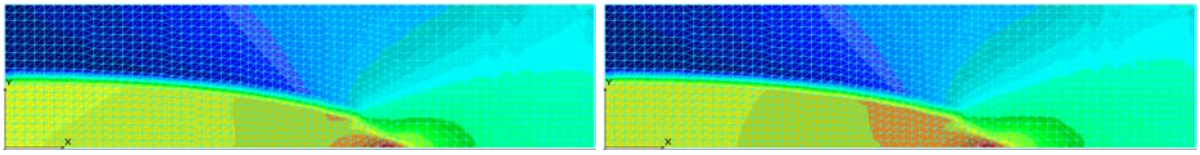

(a) normal stress σ_x (longitudinal)

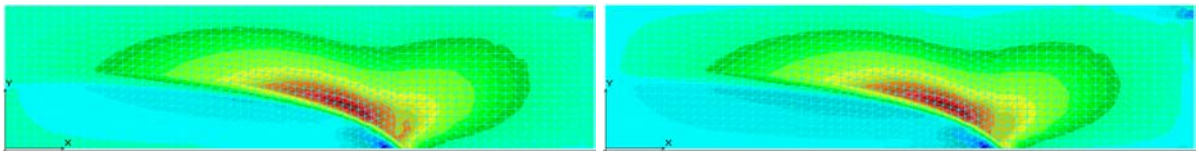

(b) shear stress τ_{xy}

Figure 6: Stress distribution in the FE model; cases of the uniform (left) or nonuniform (right) fibre distribution across the yarn.

FE modelling

To assess a possible influence of the uneven fibre distribution in the yarns on the stress field, a model FE problem is considered: 2D mesh of an elliptical impregnated yarn cross-section in a rectangular matrix domain. The uniaxial tensile load (prescribed displacement) is applied in the longest ellipse axis direction as shown in Fig. 5. Due to the symmetry, only a quarter of the structure is meshed. The properties of the fibres correspond to the ones listed in Table 1; the typical epoxy resin properties (E=3.1 GPa, G=1.2 GPa) are accepted for the matrix.

Two variants of the problem are studied: 1) even fibre distribution or 2) uneven distribution shown in Fig. 3(right). In the latter case, the cross-section is subdivided into 10 parts along the x semi-axle; each part is associated with certain fibre volume fraction. Hence, the fraction varies in a step-wise manner, and the homogenised Young's modulus decreases gradually from 10.1 GPa at the yarn core till 7.9 GPa at its edge. The average modulus of the yarn in the problem #2 is the same as the constant modulus of the impregnated yarn in the problem #1.

The results of the linear-elastic analysis are shown in Fig. 6. The overall view of the stress fields is very similar for the problems #1 and #2. However, the uniform fibre distribution results in a relatively sharp stress concentration inside and nearby the yarn tip. This fact suggests the initiation of damage at this location, which is contrary to the experimental observations. The stress fields in the case of the uneven fibre distribution are smoother (as it could be expected looking at Fig. 3) and have significantly lower (by 15–25%) maximums. Accordingly, the test data reveals no preferential crack position in the yarn cross-sections (6, 7).

CONCLUSIONS

The presented experimental study deals with the irregularity of the fibre distribution in the yarns of the braided composite preform. The main results of this preliminary study can be outlined as

- the geometrical characterization of the fabric is performed on the meso- and micro-level. A statistically significant (10–15%) variation of the local fibre volume fraction is observed along and across the yarns. They also show randomized cross-sectional shapes;

- the WiseTex software is used to build the geometrical model of the braid, including the variable fibre content inside the yarns. The model does not account for all issues of the real deformation of a dry textile in a composite processing. This would involve a description of "strange" behaviour of fibrous assemblies, frictional phenomena, etc. However, the model can serve as the base for the further FE computations (9);
- the general conclusion is that a non-negligible variability can exist in the micro- and meso-level geometry of a textile composite. More work should be done to achieve a correct FE description of the stress-strain state and homogenization of the mechanical properties.

ACKNOWLEDGEMENTS

This study was done within the I-TOOL ("Integrated Tool for Simulation of Textile Composites") project founded by the European Commission. The triaxial braided fabric used in this study has been sent by the Institut für Verbund Werkstoffe in Kaiserslautern (Germany) as part of the TECABS projects (Technologies For Carbon Fibre Reinforced Modular Automotive Body Structures). Mr. Manuël Adams, Mr. Dirk Van den Auweele, and Mr. Rudy De Vos (Dept. of Metallurgy and Materials Engineering, K.U.Leuven) are gratefully acknowledged for help with the RTM, polishing, and SEM equipment.

REFERENCES

1. Kurashiki, T. et al. Estimation of a mechanical characterization for woven fabric composites by FEM based on damage mechanics. *Proceedings of 11th European Conference on Composite Materials (ECCM-11), Rhodes, Greece, May 31–June 3, 2004*, CD edition.
2. Summerscales, J. and Russell, P.M. Observations on the fibre distribution and fibre strain in a woven fabric reinforcement. *Advanced Composite Letters*, **13**(3): 135–139 (2004).
3. Karkkainen, R.L. and Sankar, B.V. A direct micromechanics method for analysis of failure initiation of plain weave textile composites. *Composites Science and Technology*, **66**(3): 137–150 (2006).
4. John, S., Herszberg, I., and Coman, F. Longitudinal and transverse damage taxonomy in woven composite components. *Composites: Part B*, **32**: 659–668 (2001).
5. Lomov, S.V. et al. Experimental methodology of study of damage initiation and development in textile composites. *Proceedings of 27th International SAMPE Europe Conference, Paris, France, March 27–29, 2006*, CD edition.
6. Baudry, F. Damage characterization of triaxial braided textile composites. *MSc thesis*, Dept. of Metallurgy and Materials Engineering, Katholieke Universiteit Leuven, Belgium (2004).
7. Xie, H. Micro-structural and damage analysis of braided composites. *MSc thesis*, Dept. of Metallurgy and Materials Engineering, Katholieke Universiteit Leuven, Belgium (2005).
8. Grishanov, S.A. et al. The simulation of the geometry of two-component yarns. Part II: Fibre distribution in the yarn cross-section", *Journal of the Textile Institute*, **88**(4): 352–372 (1997).
9. Lomov, S.V., Ivanov, D.S., and Verpoest, I. Meso-FE modelling of 3-axial braided composites. *Proceedings of 8th International Conference on Textile Composites, Nottingham, UK, October 16–18, 2006*, CD edition.
10. Naik, R.A., Ifju, P.G., and Masters, J.E. Effect of fibre architechure parameters on deformation fields and elastic moduli of 2D braided composites. *Journal of Composite Materials*, **28**: 656–680 (1994).